subunits were found in certain segments; and (4) there could be an additional homologous subunit(s) forming a functional receptor together with the KBP. This possibility is supported by the fact that two bands were detected by northern blotting at high stringency, and that multiple proteins at positions corresponding to a M_r of 48,000 on an SDS-polyacrylamide gel were recognized by immunostaining using polyclonal and monoclonal antibodies against the KBP (refs 3, 4). Furthermore, the KBP cDNA encodes a protein that produces only a high-affinity binding site for kainate in COS-7 cells. Although the lack of the previously observed lower-affinity site[3] could be due to different post-translational modifications between frog brain and transfected COS-7 cells, it raises the possibility that a second protein, which contains the low-affinity binding site, is necessary for a physiologically functional receptor.

This study provides the first molecular characterization of a component of a kainate receptor–binding system that could be involved in EAA neurotransmission. Recent evidence has shown that EAAs are important neurotransmitters in the central nervous system and could be involved in neurotoxicity and several other neurological disorders[1,2]. This provides an impetus to characterize their receptors and related proteins. Further studies focused on isolating and expressing additional subunits of KBP should help elucidate the precise role of the protein and its relationship to neurotransmission and kainate neurotoxicity. □

Received 12 September; accepted 12 October 1989

1. Monaghan, D. T., Bridge, R. J. & Cotman, C. W. *A. Rev. Pharmac. Tox.* **29,** 365–402 (1989).
2. Foster, A. C. & Fagg, G. *Brain Res. Rev.* **7,** 103–164 (1984).
3. Hampson, D. R. & Wenthold, R. J. *J. biol. Chem.* **263,** 2500–2505 (1988).
4. Hampson, D. R., Wheaton, K. D., Dechesne, C. J. & Wenthold, R. J. *J. biol. Chem.* **264,** 13329–13335 (1989).
5. Dechesne, C. J. *et al. J. Neurosci.* (in the press).
6. Barnard, E. A., Darlison, M. G. & Seeburg, P. *Trends Neurosci.* **10,** 502–509 (1987).
7. Wada, K. *et al. Science* **240,** 330–334 (1988).
8. Saiki, R. K. *et al. Science* **239,** 487–491 (1988).
9. Kozak, M. *Nucleic Acids Res.* **12,** 857–872 (1984).
10. von Heijne, G. *Nucleic Acids Res.* **14,** 4683–4690 (1986).
11. Marshall, R. D. *Biochem. Soc. Symp.* **40,** 17–26 (1974).
12. Chen, C. & Okayama, H. *Molec. cell. Biol.* **7,** 2745–2752 (1987).
13. Munson, P. J. & Rodbard, D. *Analyt. Biochem.* **98,** 39–45 (1980).
14. Grenningloh, G. *et al. Nature* **328,** 215–220 (1987).
15. Sumikawa, K. & Miledi, R. *Proc. natn. Acad. Sci. U.S.A.* **85,** 1302–1306 (1988).
16. Kyte, J. & Doolittle, R. F. *J. molec. Biol.* **157,** 105–132 (1982).
17. Engelman, D. M., Steitz, T. A. & Goldman, A. *A. Rev. Biophys. biophys. Chem.* **15,** 321–353 (1986).
18. Schofield, P. R. *et al. Nature* **328,** 221–227 (1987).
19. Giraudat, J. *et al. Biochemistry* **26,** 2410–2418 (1987).
20. Leonard, R. J., Labarca, C. G., Charnet, P. Davidson, N. & Lester, H. A. *Science* **242,** 1578–1581 (1988).
21. Imoto, K. *et al. Nature* **335,** 645–648 (1988).
22. Kurosaki, T. *et al. FEBS Lett.* **214,** 253–258 (1987).
23. Boulter, J. *et al. Proc. natn. Acad. Sci. U.S.A.* **84,** 7763–7767 (1987).
24. Maniatis, T., Fritsch, E. F. & Sambrook, J. *Molecular Cloning: A Laboratory Manual* (Cold Spring Harbor Laboratory, New York, 1982).
25. Sanger, F., Nicklen, S. & Coulson, A. R. *Proc. natn. Acad. Sci. U.S.A.* **74,** 5463–5467 (1977).
26. Okayama, H. *et al. Meth. Enzym.* **154,** 3–28 (1987).
27. Dayhoff, M. O., Schwartz, R. M. & Orcutt, B. C. in *Atlas of Protein Sequence and Structure* Vol. 5, suppl. 3 (ed. Dayhoff, M. O.) 345–352 (National Biomedical Research Foundation, Silver Spring, Maryland, 1978).

ACKNOWLEDGEMENTS. We thank Drs J. Battey and K. Mearow for advice on PCR procedures and *in situ* hybridization, respectively. Drs J. Fex, P. Nelson and E. Freese for their support in carrying out this study and for reading the manuscript, and D. Schoenberg for her help in preparing this manuscript.

Molecular structure of the chick cerebellar kainate-binding subunit of a putative glutamate receptor

Paul Gregor, Itzchak Mano, Ilana Maoz, Michael McKeown* & Vivian I. Teichberg

Department of Neurobiology, The Weizmann Institute of Science, Rehovot 76100, Israel
* Molecular Biology and Virology Laboratory, The Salk Institute, PO Box 85800, San Diego, California 92138, USA

KAINATE receptors mediate some of the excitatory transactions carried out in the central nervous system by the neurotransmitter glutamate[1]. They are involved in neurotoxicity[2], possibly in neurodegenerative disorders[3] and it has been suggested that they have a role in long-term potentiation[4]. Kainate receptors are present both on neuronal[1] and glial[5–7] cell membranes where they regulate the gating of a voltage-independent ion channel[8]. Nothing is known about their molecular structure. Taking advantage of the unusually high abundance of ^{3}H-kainate binding sites in the chick cerebellum[9,10], we have isolated an oligomeric protein that displays a pharmacological profile similar to that of a kainate receptor, and have demonstrated, using the monoclonal antibody IX-50, that this protein is composed of a single polypeptide of M_r 49,000 which harbours the specific kainate recognition site[11]. The structure of this kainate binding protein (KBP) is also of interest because of its exclusive cerebellar localization on Bergmann glial membrane[12] in close proximity to established glutamatergic synapses[13]. We now report the isolation of the complementary DNA containing the complete coding region of the kainate binding protein. The predicted structure of the mature protein has four putative transmembrane domains with a topology analogous to that found in the superfamily of ligand-gated ion channels[14–16]. This raises the possibility, that kainate binding protein may form part of an ion channel and may be a subunit of a kainate subtype of glutamate receptor.

The chick cerebellar kainate binding protein (KBP) was isolated as previously described[11], as a single polypeptide of M_r 49K with a purity, estimated on SDS-polyacrylamide gels, of 80–95%. KBPs with similar M_r values have been isolated from frog[17] and pigeon[18] brain. Microsequencing of the N terminus of purified KBP produced only one sequence. To obtain internal amino-acid sequences of KBP, the latter was fragmented with cyanogen bromide and the five most prominent peptides (I–V), obtained on separation by reverse-phase HPLC, were submitted to N-terminal sequence analysis (P.G. and V.I.T., manuscript in preparation). All sequences determined chemically are shown (solid lines) in Fig. 1.

As peptide IV was immunopositive with monoclonal antibody IX-50 and polyclonal antibodies (data not shown) we synthesized a set of 20-nucleotide-long oligodeoxyribonucleotides (oligo(dT)) corresponding to its N terminus (probe IV; see Fig. 2 legend). To establish its suitability for screening libraries and the optimal hybridization conditions, probe IV was used to analyse RNA blots. As shown in Fig. 2*a* (panel A), probe IV hybridized mainly to a 3.9-kilobase (kb) RNA, but also to a 6-kb RNA. Both of these are much more abundant in the cerebellum than in the cerebrum and not detectable in the liver. This tissue distribution correlates very well with that of kainate-binding sites[19] and with anti-KBP immunoreactivity (data not shown). Analysis of RNA blots with probe I, derived from the sequence of peptide I, gives an identical pattern to the one shown in Fig. 2*a*, panel A.

An oligo(dT)-primed chick cerebellar cDNA library, constructed in phage λgt-10, was screened with the probe IV (for methods, see Fig. 2 legend). Positive phages were rescreened with probe I and cDNAs KBP-2.9 and KBP-2.2 were isolated. Radiolabelled KBP-2.2 cross-hybridizes to KBP-2.9 and gives the anticipated hybridization pattern on northern blots (Fig. 2*a*, panel B). Rescreening the same library with restriction fragments of cDNA KBP-2.2 resulted in isolation of the clone KBP-3.3, which has the complete coding region of KBP. The maps of clones used to establish the coding DNA sequence of KBP are shown in Fig. 2*b*.

The entire protein-coding DNA sequence and deduced

amino-acid sequence of KBP are shown in Fig. 1. The mature protein is predicted to have 464 amino acids and an M_r of 51.8K. The 23 residues preceding the N-terminal sequence probably constitute the signal peptide. The first methionine is preceded by an in-frame stop codon and has a sequence context consistent with its use as a translation start site[20]. Although we have not formally shown that the cloned cDNA expresses a protein with kainate-binding properties, several arguments indicate that the derived amino-acid sequence corresponds to that of KBP. First, the deduced amino-acid sequence contains all the peptide sequences derived from the pure 49K polypeptide harbouring the kainate-binding site[11]. Second, two of the encoded peptides (IV and V) provide determinants for polyclonal antibodies directed against KBP and peptide IV is recognized by the anti-KBP monoclonal antibody IX-50. Third, the amino-acid composition and size of the deduced sequence are, within limits of error, consistent with those of isolated KBP. Finally, the preferential cerebellar localization of the RNA species hybridizing to the cloned cDNA is strictly in line with the selective tissue distribution of KBP.

Data-base searches did not reveal any significant sequence homology of KBP to other proteins. A comparison of the overall pattern of hydrophobic residues for KBP with such patterns for known ligand-gated channels (Fig. 3), however, revealed some similarities. The KBP contains several hydrophobic regions including prominent ones near the N and C termini of the protein. In addition, there are three stretches of hydrophobicity between residues 140 and 240, each of which is long enough to span a lipid bilayer in an α-helical configuration. One interpretation of these data is that the first hydrophobic region functions as a signal peptide and that the other four regions (M1–M4) serve as membrane spanning regions. The size of KBP and the overall placement of the putative membrane spanning regions of KBP are similar to the size of known ligand-gated ion channel proteins and to the placement of putative membrane spanning regions of these proteins indicating that KBP has a general architecture similar to that of the chemically gated ion channels. If KBP resembles ligand-gated ion channels, the N and C termini are probably located extracellularly. This assignment is supported by the presence of putative N-glycosylation sites at positions 81 and 421, in the putative N- and C-terminal extracellular regions, and by the presence of putative phosphorylation sites

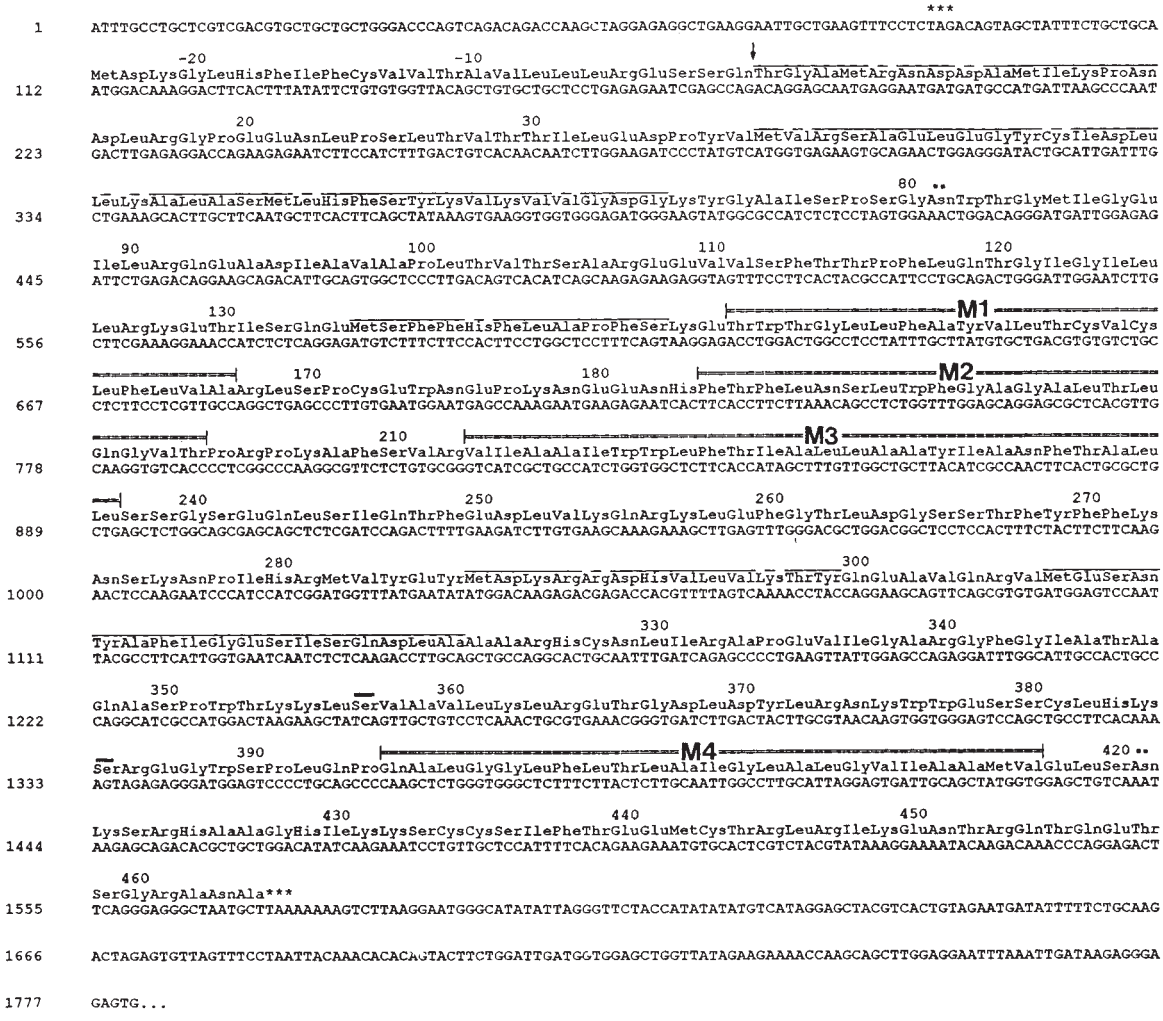

FIG. 1 DNA sequence and deduced amino-acid sequence of the chick cerebellar kainate binding protein. Nucleotides are numbered at left and amino acids above the sequence. The first in-frame stop codon in the 5′ untranslated sequence and the stop codon at the end of the coding region are labelled with asterisks. Amino-acid numbering is from the first residue of the mature N-terminal sequence as established by direct N-terminal sequencing of the kainate binding protein. The presumptive signal peptide sequence is indicated by negative numbering. Peptide sequences determined chemically are denoted by solid lines and uncertain or unidentified residues by broken lines. Signal peptide cleavage site is indicated by arrow. The proposed membrane-spanning hydrophobic sequences are indicated by double lines (M1–M4). The putative extracellular N-glycosylation sites are labelled with two dots and the putative intracellular phosphorylation sites by a solid bar.

METHODS. The cDNA inserts of positive phages were subcloned into Bluescript phagemid pKS vectors (Stratagene) and sequenced by the dideoxy chain termination method[30]. The sequence presented is combined from all cDNAs and both strands were analysed. The 3′ untranslated regions of the cDNA clones beyond the *Pst*I site were not sequenced completely on both strands and are not shown.

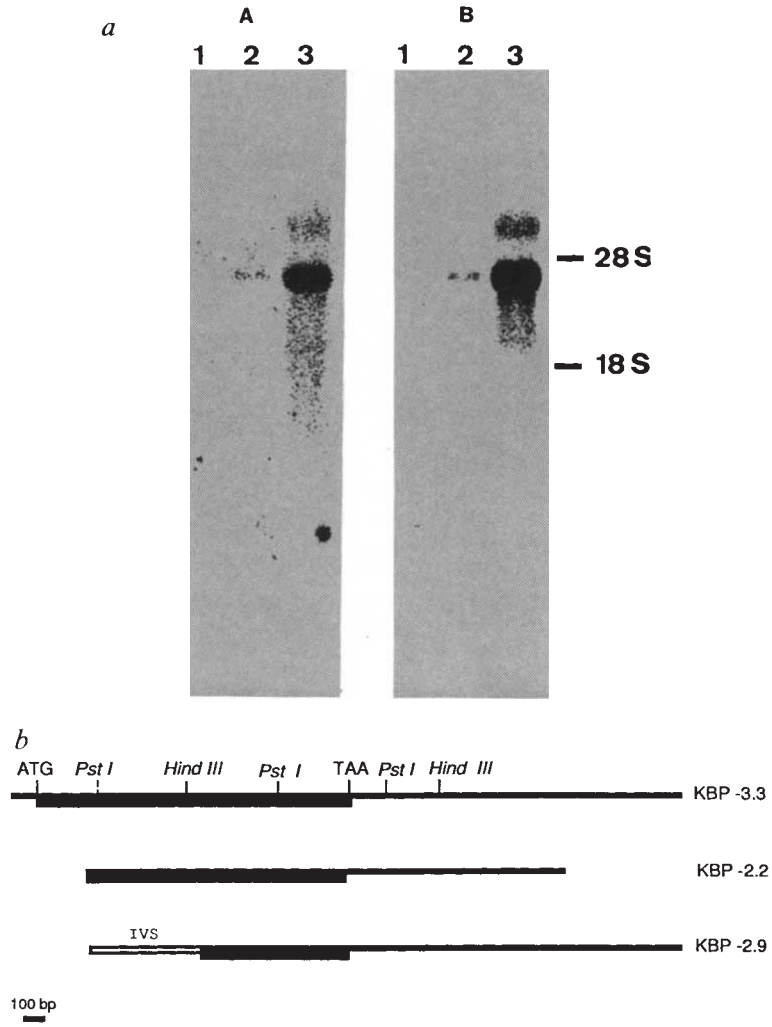

FIG. 2 Molecular cloning of the KBP cDNA. *a*, Northern blot analysis of chick RNA with oligodeoxyribonucleotide oligo-(dT) probe IV corresponding to peptide IV (panel A) and with cloned KBP-2.2 cDNA (panel B). Line 1, liver; line 2, cerebrum; line 3, cerebellum. *b*, cDNA clones and partial restriction map. All cDNAs have their cognate 3′ poly-A sequences. The 3′ untranslated region of KBP-2.2 beyond the *Hind* III site is sifferent from KBP-3.3 and KBP-2.9, probably as a result of alternate 3′-end processing. The open reading frame of KBP-2.9 was truncated at its 5′ side, probably as a result of incomplete splicing. Solid box, protein coding region, IVS, presumed intervening sequence.

METHODS. Standard recombinant DNA methods were as described[25]. Based on the sequence of peptide IV, the oligo-(dT) 5′-AARGCGTAGTTGSWCTCCAT-3′ (where R=A or G, S=C or G, W=A or T)[26] was synthesized (probe IV) and labelled to high specific radioactivity with [γ^{32}P]ATP[27]. Total RNA was isolated[28] from adult chick tissues; 25 μg per line was electrophoresed on a 1% formaldehyde agarose gel, blotted on nitrocellulose membrane (Hybond-C, Amersham) and hybridized overnight with the radiolabelled oligo-(dT) probe at 37 °C in 5×SSPE (1×SSPE contained 0.18 M NaCl, 0.01 M sodium phosphate, 1 mM EDTA, pH 6.8) as described[27]. The high stringency wash was at 37 °C in 0.5×SSPE for 1 h. Antisense probe I based on peptide I sequence was synthetized as an oligonucleotide mixture 5′-TAIGTIACIACIAGIACRTGRTCICAIC-QCTTRTTC-3′ (where I=inosine, Q=G or T and R=A or G), and radiolabelled as above. To isolate KBP cDNAs, an oligo-(dT)-primed cDNA library in phage λgt-10 (ref. 29) was constructed from cerebellar poly(A)$^+$-RNA of hatching chicks. Double-stranded cDNA was synthesized, fitted with *Eco*RI linkers, and cDNAs were size fractionated on 1% agarose gel. Fragments larger than 1.5 kb were isolated and ligated with *Eco*RI cut λgt-10, resulting in 150,000 independent recombinants of which at least 50% carried inserts. The library was amplified and ~160,000 phages screened with probe IV as described above; positives were rescreened with probe I resulting in isolation of KBP-2.9 and KBP-2.2 clones. A screen of 300,000 phages, under high stringency conditions, with the 0.8 kb *Pst*I–*Pst*I and 0.1 kb *Eco*RI–*Pst*I fragments derived from the 5′ end of KBP-2.2, led to the isolation of the clone KBP-3.3

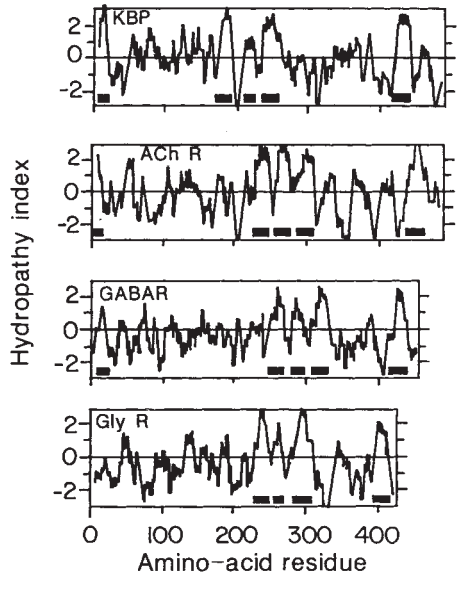

FIG. 3 Structural similarity of the KBP to subunits of ligand-gated ion channels. Hydropathy profiles computed according to Kyte and Doolittle[31], averaged over a window of 9 residues and plotted with a 1-residue interval. Solid box, putative signal peptide and membrane spanning regions. AChR, α2 chick acetylcholine receptor subunit[32]; GABA R, γ-amino-butyric acid receptor α subunit[15]; Gly R, glycine receptor[16].

at positions 357 and 385, in the putative intracellular region between M3 and M4.

Further analysis of KBP structure shows the presence of features compatible with channel function, particularly in its putative M2 transmembrane segment. Indeed, the M2 domain of the various nicotinic acetylcholine receptor (AChR) subunits[14], which is essential to channel function[21–23], contains polar uncharged residues and is preceded by hydrophilic negatively charged residues. Similar features in the equivalent region of KBP are observed, indicating, only by analogy, a possible role in ion permeation. As mentioned above, KBP also contains potential phosphorylation sites, a finding consistent with the reported modulation of kainate-gated currents by protein kinase[24]. If indeed, KBP forms part of an ion channel, its sequence does not display the homologies that have been used to group the various chemically gated ion channels in a single family. The structure of KBP must therefore reflect its idiosyncratic properties, one of which is its unusually high density in the cerebellum and exclusive presence on Bergmann glia (ref. 12 and P. Somogyi, N. Eshhar, V.I.T. & J. D. Roberts, unpublished observations). Although its function is not yet known, its localization on Bergmann glial membranes surrounding the parallel fibre—Purkinje cell glutamatergic synapse indicates a role in modulation of synaptic efficacy. Of relevance are our recent findings that isolated Bergmann glial cells in culture display high levels of KBP, depolarize in response to kainate and release GABA (γ-aminobutyric acid) (ref. 12 and A. Ortega and V.I.T., unpublished observations). The structural data presented here, together with the above observations, indicate therefore that KBP may be a subunit of a glial subtype of kainate receptor/cation channel. □

Received 18 October; accepted 14 November 1989.

1. Watkins, J. C. & Evans, R. H. *A. Rev. Pharmacol. Tox.* **21,** 165–204 (1981).
2. Fuxe, K., Roberts, P. & Schwarcz, R. (eds) *Excitotoxins* (Plenum, New York, 1983).
3. Cotman, C. W. & Monaghan, T. *Adv. exp. Med. Biol.* **203,** 237–252 (1986).
4. Collingridge, L. & Bliss, T. V. P., *Trends Neurosci.* **10,** 288–293 (1987).
5. Bowman, C. L. & Kimelberg, H. K. *Nature* **311,** 656–659 (1984).
6. Sontheimer, H., Kettenmann, H., Backus, K. H. & Schachner, M. *Glia,* **1,** 328–336 (1988).
7. Usowicz, M. M., Gallo, V. & Cull-Candy, S. G. *Nature* **339,** 380–383 (1989).
8. O'Brien, R. & Fischbach, G. D. *J. Neurosci.* **6,** 3275–3283 (1986).
9. London, E. D., Klemm, N. & Coyle, J. T. *Brain Res.* **192,** 463–476 (1980).
10. Henke, H. & Cuenod, M. in *Neurotransmitters and Their Receptors* (eds Littauer, U. Z. *et al.*) 373–390 (Wiley, New York, 1980).
11. Gregor, P., Eshhar, N., Ortega, A. & Teichberg, V. I. *EMBO J.* **7,** 2673–2679 (1988).
12. Teichberg, V. I. *et al.* in *Excitatory Amino Acids and Neuronal Plasticity* (ed. Y. Ben Ari) (Plenum, New York, in the press).
13. Blackstone, C. D., Supattapone, S. & Snyder, S. H. *Proc. natn. Acad. Sci. U.S.A.* **86,** 4316–4320 (1989).
14. Numa, S. *Harvey Lectures* **83,** 121–165 (1989).
15. Schofield, P. *et al. Nature* **328,** 221–227 (1987).
16. Grenningloh, G. *et al. Nature* **328,** 215–220 (1987).
17. Hampson, D. R. & Wenthold, R. J. *J. biol. Chem.* **263,** 2500–2505 (1988).
18. Klein, A. U., Niederoest, B., Winterhalter, K. H., Cuenod, M. & Streit, P. *Neurosci. Lett.* **95,** 359–364 (1988).
19. Eshhar, N. *et al. Brain Res.* **476,** 57–70 (1989).
20. Kozak, M. *Nucleic Acids Res.* **15,** 8125–8132 (1987).
21. Imoto, K. *et al. Nature* **335,** 645–648 (1988).
22. Leonard, R. J., Labarca, C. G., Charnet, P., Davidson, N. & Lester, H. A. *Science* **242,** 1578–1581 (1988).
23. Miller, C. *Neuron* **2,** 1195–1205 (1989).
24. Liman, E. R., Knapp, A. G. & Dowling, J. E. *Brain Res.* **481,** 399–402 (1989).
25. Maniatis, T., Fritsch, E. F. & Sambrook, J. *Molecular Cloning: A Laboratory Manual* (Cold Spring Harbor Laboratory, New York, 1984).
26. Lathe, R. *J. molec. Biol.* **183,** 1–12 (1985).
27. Meinkoth, J. & Wahl, G. *Analyt. Biochem.* **138,** 267–284 (1984).
28. Cathala, G. *et al. DNA* **2,** 329–335 (1983).
29. Huynh, T. V., Young, R. A. & Davis, R. W. in *DNA Cloning: A Practical Approach* Vol. 1 (ed. Glover, D. M.) 49–78 (IRL, Oxford, 1985).
30. Sanger, F., Nicklen, S. & Coulson, A. R. *Proc. natn Acad. Sci. U.S.A.* **74,** 5463–5467 (1977).
31. Kyte, J. & Doolittle, R. F. *J. molec. Biol.* **157,** 105–132 (1982).
32. Nef, P., Oneyser, C., Alliod, Ch., Couturier, S. & Ballivet, M. *EMBO J.* **7,** 505–601 (1988).

ACKNOWLEDGEMENTS. We thank Natan Tal, David Ornstein and Chevi Lamed for technical assistance. This work was supported by the Leo and Julia Forcheimer Center of Molecular Genetics at the W.I.S. and by N.I.H. (M.McK).

Specificity pockets for the side chains of peptide antigens in HLA-Aw68

T. P. J. Garrett*, M. A. Saper*, P. J. Bjorkman†, J. L. Strominger & D. C. Wiley*‡

Department of Biochemistry and Molecular Biology and *Howard Hughes Medical Institute, Harvard University, Cambridge, Massachusetts 02138, USA

We have determined the structure of a second human histocompatibility glycoprotein, HLA-Aw68, by X-ray crystallography and refined it to a resolution of 2.6 Å. Overall, the structure is extremely similar to that of HLA-A2 (refs 1, 2; and M.A.S. *et al.*, manuscript in preparation), although the 11 amino-acid substitutions at polymorphic residues[3,4] in the antigen-binding cleft[2] alter the detailed shape and electrostatic charge of that site. A prominent negatively charged pocket within the cleft extends underneath the α-helix of the α_1-domain, providing a potential subsite for recognizing a positively charged side chain or peptide N terminus. Uninterpreted electron density, presumably representing an unknown 'antigen(s)', which seems to be different from that seen in the HLA-A2 structure[1], occupies the cleft and extends into the negatively charged pocket in HLA-Aw68. The structures of HLA-Aw68 and HLA-A2 demonstrate how polymorphism creates and alters subsites (pockets) positioned to bind peptide side chains, thereby suggesting the structural basis for allelic specificity in foreign antigen binding.

HLA-Aw68 (formerly HLA-A28) is the product of one allele of the polymorphic HLA-A locus of the major histocompatibility complex (MHC). Like other class I histocompatibility glycoproteins HLA-Aw68 seems to form complexes with peptides derived from internal degradation of self and nonself antigens[5–8]. These complexes are recognized on cell surfaces by cytotoxic T lymphocytes (CTL) leading to the elimination of virally infected or histoincompatible cells. The extensive polymorphism of histocompatibility glycoproteins is concentrated at the putative peptide-binding cleft[2,9], indicating that the variability was selected to generate diversity in peptide binding and T-cell receptor recognition[2]. Individual class I and class II histocompatibility glycoproteins interact with an extremely broad range of peptides of diverse sequences[10–14], yet exhibit selectivity by failing to interact with many peptides. This failure to interact probably

† Present address: Division of Biology, Howard Hughes Medical Institute, California Institute of Technology, Pasadena, California, USA.
‡ To whom correspondence should be addressed.

FIG. 1 Comparison of HLA-Aw68 and HLA-A2. *a*, Main-chain ribbon diagram of HLA-Aw68 with the 13 side chains of residues that differ from those of HLA-A2. Ten differences between HLA-A2 and HLA-Aw68, respectively, (F9Y, E63N, K63N, H70Q, H74D, V95I, R97M, H114R, Y116D and L156W) are in the binding cleft. One difference, G62R, faces up from the α_1-domain α-helix (labelled 62). W107G (labelled 107) is on a loop in the α_2-domain and A254V (labelled 245) is on the α_3-domain. β_2-microglobulin is red. *b*, Stereoview of HLA-Aw68 and HLA-A2 showing the α-carbon atoms of the α_1- and α_2-domains superimposed. Side-chain differences in HLA-Aw68 are in solid lines. Root-mean-square differences between atomic positions of α-carbons (with $B \leq 35$ Å^2) in HLA-Aw68 and HLA-A2: domains α_1 and α_2, 0.45 Å; α_3-domains, 0.27 Å; and β_2-microglobulin, 0.30 Å; Standard deviation (s.d.) of overall coordinate errors in each structure are estimated at 0.3 Å (for further details, see refs 18, 19, and M.A.S. *et al.*, manuscript in preparation). (In the site only a few small shifts in main-chain positions (over 2 s.d. of the error) are observed, one in the α-helix of α_1-domain at residues 61–71, another in the α-helix of α_2-domain in the region 148–156, and a third in a β-strand at positions 97, 98 and 101 (Fig. 1*b*).) For details of structure determination, see ref. 18. Briefly, the initial model was based on the structure of HLA-A2 at 3.0 Å. Side-chains that differed between the two molecules were fit in electron density maps calculated with coefficients F_o (Aw68) and F_o (Aw68) − F_o(A2) and phases calculated from the HLA-A2 model. The structure was refined using the program, XPLOR[30,31]; current *R* factor = 17.9% for all data; $I > 1\sigma$; 6–2.6 Å; 7 water molecules; r.m.s. deviations from ideal bond lengths, 0.016 Å; angles, 3.5°. When residues that differ between HLA-Aw68 and HLA-A2 were omitted, difference maps showed clear electron density for the ten residues pointing into the site and for 245. Density for Gly 107 and the side-chain of Arg 62 appeared weak owing to disorder. An analysis of the effect of crystal contacts on the structures of HLA is found in ref. 17. *a*, Prepared with HYDRA (R. Hubbard, unpublished); *b*, Prepared with PLUTO (S. Motherwell, E. Dodson and P. Evans, unpublished). Single-letter amino-acid code.

FIG. 4 Sections perpendicular to the length of the cleft showing different and similar pockets in HLA-Aw68 and HLA-A2 binding sites. *a*, *c*, *d*, Sections through solvent contact surfaces coloured by charge: red, acidic; blue, basic; green, His; yellow, neutral. The cleft appears as a central depression; the α_1-domain α-helix is towards the top right, the α_2-domain α-helix is at the top left; β-sheet residues form the bottom of the groove. *a*, A pocket at Asp 74 under the α_1-domain α-helix of HLA-Aw68. Note red 'dots' on the top of the pocket indicate the surface is formed by the carboxylate oxygens of Asp, 74. *b*, Same view of HLA-Aw68 as in *a* showing extra electron density (red) which fills the cleft, reaching into the '74 pocket'. Picture is sectioned through a blue van der Waal's surface of HLA-Aw68 and has a yellow α-carbon backbone. *c*, The pocket at Met 45 of HLA-Aw68 extends under the α_1-domain α-helix. *d*, The pocket at Met 45 HLA-A2 is similar to that in *c*. Note also the essentially identical structure of HLA-Aw68 and HLA-A2 in regions where atoms are labelled in red. (Label: Sequence number, atom type). The extra electron density bound to HLA-Aw68 is not currently interpretable as a single conformation such as an α-helix. Figures constructed using HYDRA (R. Hubbard, unpublished) and MS (ref. 29).